

Artificial Neural Network–Based Design and Optimization of a Rectangular Patch Antenna for 5G Mid-Band Applications



*¹Olaosebikan Akanni Aremu, ²Sheu Akeem Lawal, ¹Oluniyi Samuel Makinde,
³Mufutau Jelili Adekunle and ⁴Michael Olusope Alade

¹Department of Physics with Electronics, The Polytechnic, Ibadan, Nigeria

²Department of Physics, Emmanuel Alayande University of Education, Oyo, Nigeria.

³General Studies Department, Federal School of Surveying, Oyo, Nigeria.

⁴Department of Pure and Applied Physics, Ladoke Akintola University of Technology, Ogbomoso, Nigeria.

*Corresponding authors' email: aremurichard@yahoo.com

ABSTRACT

This paper presents the design and simulation of a low-profile patch antenna for 5G mid-band applications (3.5 GHz). The substrate material selected is Rogers RT/Duroid 5880 epoxy, which has a permittivity of 2.2. The proposed antenna layout is simulated using Computer simulation Technology (CST) Microwave Studio Suite. The simulation results indicate significant variations in S11, gain, directivity, efficiency, and bandwidth due to differences in the substrate's relative permittivity and thickness. The designed antenna achieved a return loss of -43.85 dB, VSWR of 1.015, gain of 32 dBi, directivity of 33.9 dBi, bandwidth of 177 MHz, and efficiency of 94%. With a gain exceeding 5 dBi, the antenna is well-suited for communication applications. The paper also develops a mathematical model employing the Multivariate Polynomial algorithm to predict three antenna parameters: Return Loss, VSWR, and Bandwidth. An artificial neural network-based model has been developed using the Levenberg-Marquardt algorithm with a feed-forward back-propagation learning approach and applied to patch antenna design. It processes input data, including the dielectric constant (ϵ_r), substrate thickness (hs), and dominant-mode resonant frequency (fr), to predict the S11, VSWR, and Bandwidth. The model's performance has been evaluated by comparing its results with simulated values obtained from CST Studio Suite. The machine learning predictions closely align with the simulation results. Additionally, the neural network-based estimation offers the advantage of rapid and simultaneous output computation.

Keywords:

Antenna,
Bandwidth,
Machine learning,
Optimization,
Return loss,
VSWR.

INTRODUCTION

Microstrip antennas are widely used in mobile communication applications that require multiband and/or wideband frequency operations, high power gain, and omnidirectional radiation patterns. Consequently, designing printed antennas to accommodate multiple operational services is a challenging task. This necessitates highly accurate calculations of various design parameters for microstrip patch antennas. The dimensions of a rectangular microstrip patch antenna play a crucial role in determining its performance and effectiveness. In this study, microstrip line feeding is chosen as the preferred method for delivering input power to the antenna. Precisely calculating the patch dimensions is especially critical when the antenna size is

significantly compact. Several studies have been published on the calculation of microstrip antenna patch dimensions (Aremu et. al., 2025; Narayan et. al., 2019). However, these studies exhibit significant deviations in the computed patch dimensions when compared to theoretical and simulation results. It is possible to use the machine learning models for optimization that is both effective and accurate, and these models can be generated within the range of training (Poornima and vInod 2017). Exploiting the feed forward network permitted for the successful completion of the task of estimating the S11, VSWR, and bandwidth of the flexible antenna. Machine learning have recently gained attention as a fast and flexible tool for modeling, simulations and optimization of microstrip patch

antenna. Recently CAD approach based on neural networks has been introduced in the microwave community for modeling of passive and active microwave component. Several research papers (Patnaik et. al., 2017; Karaboga et. al., 1999) indicates how Machine learning can be used efficiently to calculate different design and performance parameters of microstrip antennas. Nevertheless, the literature (Sagiroglu et. al., 2003) shows that only three-layer MLPFFBP has been preferred to prove the utility of ANN in the area of microstrip antenna design. This study therefore, explores the potential of machine learning techniques to determine the length (L) and width (W) of a microstrip patch antenna on a ground plane, considering a substrate thickness (h) and dielectric constant (ϵ_r).

Design and Data Generation

This section outlines the materials and methodology used in the antenna design process. A Rogers's substrate was selected for this design. Initially, CST software was utilized for modeling the antenna, with the substrate material being one of the key design requirements. The antenna's performance will then be evaluated by comparing the results with previously published findings. If the obtained results are unsatisfactory, optimization will be carried out until the desired performance is achieved. The design process begins with estimating the antenna's length (L_p), width (W_p), and the ground plane dimensions (L_g and W_g). These calculations were performed using equations (1–9) to achieve the required values (Ghazaoui et. al., 2020; Abdulbari et. al., 2021). Following this, modifications are applied to refine the design and obtain the most optimal results. Subsequently, modifications are applied to achieve the most optimal results. The material properties used in the antenna design include a substrate thickness of 0.27 mm, a dielectric constant (ϵ_r) of 2.2, a loss tangent ($\tan \delta$) of 0.0009, and a patch thickness of 0.037 mm.

Step 1: Calculation of the Patch Width (W_p)

In this study, the detailed procedure and design equations (Hossain et. al., 2021; Rahman et. al., 2022) for the proposed single element Microstrip patch antenna designed at the operating frequency 3.5 GHz for 5G applications using Rogers RO3000 substrate are as follows $f_r = 3.5 \times 10^9$ Hz, $c = 3 \times 10^8$ ms⁻¹, $h = 1.6$ mm and $\epsilon_r = 2.2$. The patch width (W_p) of the antenna is computed based on (1) as:

$$W_p = \frac{c}{2f_r \sqrt{\frac{\epsilon_r + 1}{2}}} \quad (1)$$

Step 2: Design of Effective Dielectric Constant, ϵ_{eff}

The effective dielectric constant ϵ_{eff} introduced to account for the fringing and the wave propagation in the line. ϵ_{eff} is obtained from (2)

$$\epsilon_{eff} = \frac{\epsilon_r + 1}{2} + \frac{\epsilon_r - 1}{2} \left(1 + 12 \frac{h}{W}\right)^{-0.5} \quad (2)$$

Step 3: Design of Effective and Actual Length of the patch

The effective length of the patch is calculated from (3)

$$L_{eff} = \frac{c}{2f_r \sqrt{\epsilon_{eff}}} \quad (3)$$

The length extension (ΔL) is subtracted from the length of the patch with actual length of the patch unchanged. The length extension is considered due to fringing field as seen in

(4) while the actual length of the patch is obtained using (5)

$$\Delta L = 0.412h \frac{(\epsilon_{eff} + 0.3) \left(\frac{W}{h} + 0.264\right)}{(\epsilon_{eff} - 0.258) \left(\frac{W}{h} + 0.8\right)} \quad (4)$$

$$L_p = L_{eff} - 2\Delta L \quad (5)$$

Step 4: Design of Ground Plane Dimensions (L_g and W_g)

The length and width of the ground is computed using (6) and **Error! Reference source not found.** respectively as:

$$L_g = 6h + L_p \quad (6)$$

$$W_g = 6h + W_p \quad (7)$$

Step 5: Feedline Designed

For a 50 Ω microstrip feedline, the characteristic impedance equation is used as,

$$Z_0 = \frac{60}{\sqrt{\epsilon_{eff}}} \ln \left(\frac{8h}{W_f} + \frac{W_f}{4h}\right) = 3.33 \text{ mm} \quad (8)$$

The feedline length is chosen based on practical layout constraints and should be long enough to allow proper impedance matching. The expression is given by,

$$L_f = \frac{\lambda_g}{4} \quad (9)$$

where the guided wavelength is given as, $\lambda_g = \frac{\lambda_0}{\sqrt{\epsilon_{eff}}}$

For 3.5 GHz frequency and $c = 3 \times 10^8$ ms⁻¹, free space wavelength $\lambda_0 = 85.7$ mm. Hence, the value of λ_g and L_f are determined.

Step 6: Computation of Antenna Efficiency (η) and Reflection Coefficient (Γ)

Antenna efficiency (η) is determined by converting the gain (G) and directivity (D) obtained after simulation into linear scale, the relationship is as shown in (10)

$$\eta = \frac{10^{(G_{dBi}/10)}}{10^{(D_{dBi}/10)}} \quad (10)$$

The Reflection Coefficient (Γ) quantifies how much of the incident power is reflected due to impedance mismatch. It is related to S11 by (11),

$$\Gamma = 10^{S_{11}/20} \tag{11}$$

The reflected power (P_r) presents the percentage of incident power that is reflected due to impedance mismatch, it is computed using the expression given by (12)

$$P_r = \Gamma^2 \times P_{iincident} \tag{12}$$

The power radiated by the antenna can be estimated by subtracting the power reflected from antenna input power, equivalently as shown in (13)

$$P_{radiated} = (1 - |\Gamma|^2) \cdot P_{input} \tag{13}$$

where Γ is the linear reflection coefficient given as (14),

$$\Gamma = 10^{RL/20} \tag{14}$$

Table 1 shows the design specification of the proposed antenna while

Table 2 presents the dimensions of the optimized antenna designed.

Table 1: Design Specifications of the Proposed Antenna

Parameter	W_p	L_p	W_g	L_g	ϵ_r	h	t	W_f	L_f
Dimensions (mm)	38.2	28.3	47.9	37.9	2.2	1.6	0.035	3.1	16.0

Table 2: Dimension of the Optimized Antenna Design

Parameter	Value
Resonant frequency (f_r)	3.5 GHz
Patch width (W_p)	26.2 mm
Patch length (L_p)	18.7 mm
Length of ground (L_g)	29.7 mm
Width of ground (W_g)	35.8 mm
Substrate height (h)	1.6 mm
Dielectric constant (ϵ_r)	2.20
Feedline Width (W_f)	2.27 mm
Feedline length (L_f)	16.0 M

Optimization of Antenna Designed

The optimization method will concentrate on two design parameters—substrate height (h_s) and patch length (L_p)—selected based on the antenna designed in the previous section. Variations in these parameters significantly influence the antenna’s performance during optimization. Multiple simulations are conducted, testing various values to generate datasets for experimentation and mathematical modeling. After developing a suitable model, the parameters are fine-tuned using a constrained numerical method to achieve the desired performance level. The enhanced antenna performance is then validated through simulations in Computer Simulation Technology (CST) software, which utilizes an electromagnetic solver. Table 3 presents the variations in antenna performance along with detailed parameter values.

Machine Learning Back Propagation Technique

In this study, the ANN model was trained using dielectric constant, substrate, thickness and cutoff frequencies as inputs, with patch length and width. back propagation was employed to minimize the error between predicted and actual resonant frequencies, ensuring that the forward and inverse models consistently yield accurate patch dimensions for a desired resonant frequency.

Treatment of Data and Development of Artificial Neural Network

A minimum-maximum normalization process was performed on the inputs and preprocessed path loss dataset obtained along the three itineraries using (16). This was done to prevent impulsive changes due to large variation in the datasets

$$y = \frac{(y_{max} - y_{min}) \times (x_{in} - x_{min})}{(x_{max} - x_{min})} + y_{min} \tag{15}$$

Since $y_{min} = -1$ and $y_{max} = +1$, x_R is the original data, y is the result of normalization. Equation (15) becomes (16),

$$y = \frac{2(x_{in} - x_{min})}{(x_{max} - x_{min})} - 1 \tag{16}$$

The normalized dataset was processed using a single-layer feed forward back propagation neural network trained with the Levenberg–Marquardt algorithm. The data were randomly partitioned into 70% for training, 15% for validation, and 15% for testing. All simulations were performed using MATLAB 2024a (MathWorksInc.). The artificial neural network architecture is illustrated in Figure 1 and Figure 2.

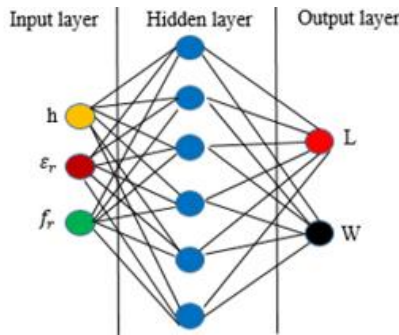


Figure 1: Forward Propagation ANN Model for 3×6×1 Architecture

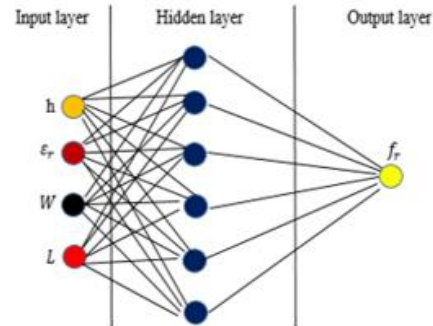


Figure 2: Backward Propagation ANN Model for 3×6×1 Architecture

Machine Learning Modeling

A tansig activation function was employed in the hidden layer and a purelin function in the output layer, as described in Eq. 17.

$$y = \sum_{j=1}^m \{ \text{Purelin} [LW_{j,1} (\sum_{i=1}^4 \text{tansig}(X_i IW_{i,j} + b_j))] \} + b_o \quad (17)$$

The network was trained using 1,000 epochs and a zero-error goal as stopping criteria. Following

denormalization, the model’s performance was assessed by comparing actual and predicted values using correlation coefficients (R-values) for S11, VSWR, and bandwidth. As shown in Table 3, the model demonstrated excellent predictive accuracy for S11 and VSWR, with slightly lower yet satisfactory performance for bandwidth.

Table 3: R-values for Trained Data

Antenna characteristics	Training	Validation	Test	All
S11	0.9967	1.0000	1.0000	0.9667
VSWR	1.0000	1.0000	1.0000	0.9443
Bandwidth	1.0000	1.0000	1.0000	0.8995

Polynomial Regression Model

A polynomial regression model for the two independent variables (x_1, x_2), and one dependent variable (y) is expressed as (18),

$$y = \beta_0 + \beta_1 x_1 + \beta_2 x_2 + \beta_3 x_1^2 + \beta_4 x_2^2 + \beta_5 x_1 x_2 + \epsilon \quad (18)$$

where β_0 is the intercept, β_1 and β_2 are the linear coefficients, β_3 and β_4 are the quadratic coefficients, β_5 is the interaction term coefficient, and ϵ is the error term. In this study, the second order polynomial (19) with two independent variables $x_1=f_r$ and $x_2=h_s$ is given as,

$$y = \beta_0 + \beta_1 f_r + \beta_2 h_s + \beta_3 f_r^2 + \beta_4 h_s^2 + \beta_5 f_r h_s + \epsilon \quad (19)$$

The attained regression equation for the return loss (S11) is presented as (20):

$$y = 4032 + (-1678.5 * f_r) + (-1222.4 * h_s) + 235 * f_r^2 + (-11.6 * f_r * h_s) + (872 * h_s^2) \quad (20)$$

The regression equation obtained for VSWR is (21):

$$y = 25.9 + (-12.2 * f_r) + (-3.28 * h_s) + (1.72 * f_r^2) + (-0.18 * f_r * h_s) + (1.15 * h_s^2) \quad (21)$$

The regression equation obtained for Bandwidth is (22):

$$y = -4808 + (1865 * f_r) + (2065 * h_s) + (-307.3 * f_r^2) + (197.2 * f_r * h_s) + (-832.4 * h_s^2) \quad (22)$$

RESULTS AND DISCUSSION

Figures 3, 4, and 5 present 3D plots illustrating the influence of resonant frequency (f_r) and substrate height (h_s) on S11, VSWR, and bandwidth. The results reveal that S11 exhibits a non-linear relationship with both f_r and h_s , with darker regions on the color map indicating improved impedance matching (lower S11 values). Figure 3: highlights that minor variations in h_s significantly influence return loss. As shown in Figure 4,

VSWR also follows a non-linear trend with increasing f_r , with measured values aligning well with the predicted surface. Regions with higher VSWR values indicate poorer impedance matching. Figure 5 illustrates the variation of bandwidth, which shows a mixed trend—expanding in certain regions and narrowing in others. The influence of f_r on bandwidth is more pronounced than that of h_s , suggesting frequency sensitivity in determining antenna performance.

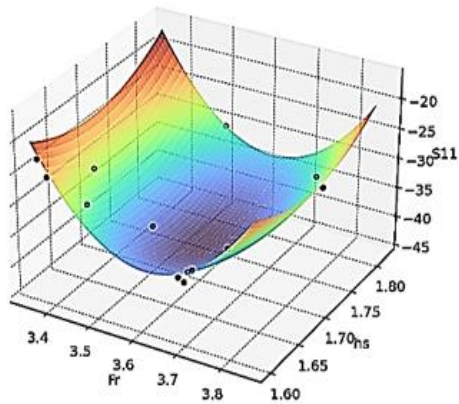


Figure 3: 3D Outlook of Polynomial Regression fit for S11

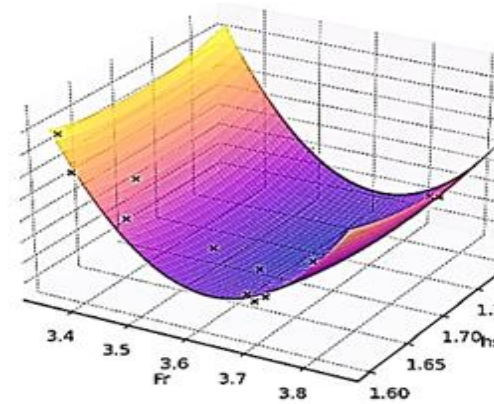


Figure 4: 3D outlook of Polynomial Regression fit for VSWR

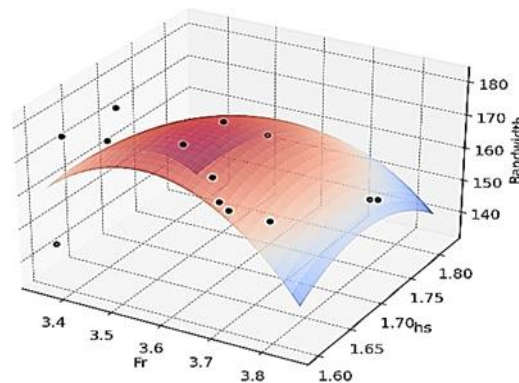


Figure 5: 3D Outlook of Polynomial Regression fit for Bandwidth

Table 4 compares the original and predicted values of the antenna performance metrics across thirteen samples. The results demonstrate a strong correlation between the actual and predicted data, confirming the reliability of the model and the effectiveness of the derived regression equations in estimating the target parameters.

Table 5 presents the numerical relationship between substrate height (h_s) and bandwidth based on test

samples. While not strictly linear, the trend indicates that bandwidth generally increases with h_s . It was noted that, at $h=1.61$ mm, bandwidth starts at 145.13 MHz, then increases at different heights, reaching a maximum of 180.93 MHz at $h=1.65$ mm.. This behavior suggests that moderate increases in substrate height may enhance bandwidth due to improved impedance matching and reduced surface wave losses.

Table 4: Comparison between Original and Predicted Values of the Performance Metrics

f_r (GHz)	L_g (mm)	δ	h_s (mm)	W_g (mm)	W_p (mm)	L_p (mm)	ϵ_r	S11 (dB)	VSWR	Bandwidth (MHz)
3.351	29.7	0.009	1.61	35.8	26.2	20.11	2.2	-23.09	1.155	143
3.505	29.7	0.009	1.82	35.8	26.2	20.19	2.2	-30.79	1.062	153
3.852	29.7	0.009	1.72	35.8	26.2	20.21	2.2	-26.42	1.104	159
3.802	29.7	0.009	1.75	35.8	26.2	19.99	2.2	-28.05	1.084	153
3.755	29.7	0.009	1.63	35.8	26.2	20.04	2.2	-30.96	1.075	162
3.715	29.7	0/009	1.60	35.8	26.2	19.97	2.2	-32.73	1.052	168
3.670	29.7	0.009	1.62	35.8	26.2	20.13	2.2	-37.52	1.031	166
3.630	29.7	0.009	1.64	35.8	26.2	19.98	2.2	-39.39	1.022	169
3.505	29.7	0.009	1.69	35.8	26.2	20.12	2.2	-43.85	1.015	177
3.545	29.7	0.009	1.66	35.8	26.2	20.00	2.2	-34.28	1.046	173
3.465	29.7	0.009	1.61	35.8	26.2	19.97	2.2	-28.22	1.089	178

3.425	29.7	0.009	1.65	35.8	26.2	20.10	2.2	-26.31	1.103	181
3.388	29.7	0.009	1.60	35.8	26.2	20.21	2.2	-24.55	1.128	178

Table 5: Comparison of Original and Predicted Antenna Parameters

F (GHz)	h_s (mm)	S11 original	S11 predicted	VSWR original	VSWR predicted	Bandwidth original	Bandwidth predicted
3.351	1.61	-23.098	-22.01	1.155	1.085	143	145.13
3.505	1.82	-30.798	-30.798	1.062	1.094	153	153.79
3.852	1.72	-26.423	-26.423	1.104	1.104	159	161.33
3.802	1.75	-28.059	-28.059	1.084	1.084	153	159.39
3.755	1.63	-30.965	-30.965	1.075	1.075	162	167.06
3.715	1.60	-32.731	-34.560	1.052	1.052	168	166.79
3.670	1.62	-37.527	-37.527	1.031	1.031	166	168.15
3.630	1.64	-39.399	-37.772	1.022	1.022	169	170.30
3.505	1.69	-43.850	-46.980	1.015	1.015	177	175.76
3.545	1.66	-34.285	-34.285	1.046	1.046	173	176.07
3.465	1.61	-28.223	-28.223	1.089	1.038	178	176.29
3.425	1.65	-26.316	-26.316	1.103	1.103	181	180.93
3.388	1.60	-24.551	-24.551	1.128	1.134	178	179.65

Return Loss (S11)

Figure 6 illustrates the return loss (S11) values across various frequencies for the trained dataset, considering different substrate heights. The frequency range spans from 3.351 GHz to 3.852 GHz, with corresponding return loss values between -22.02 dB and -46.98 dB. The minimum return loss of -46.98 dB is observed at 3.585 GHz, indicating optimal impedance matching at this frequency. Frequencies between 3.63 GHz and 3.67 GHz also exhibit high return loss values (below -37 dB), suggesting a broad region of efficient antenna performance. Conversely, higher return loss values—such as -22.02 dB at 3.351 GHz and -24.55 dB at 3.388 GHz—indicate relatively poorer matching at those

frequencies. Overall, the results confirm that the trained model accurately predicts the frequency range with optimal impedance characteristics, with peak performance centered around 3.585 GHz.

Figure 7 presents the variation of the machine learning-predicted VSWR across the frequency range. The VSWR values remain consistently close to 1, indicating effective impedance matching throughout. The minimum VSWR of 1.015 occurs at 3.585 GHz, signifying optimal matching, while the maximum value of 1.134 at 3.388 GHz still falls within acceptable limits for efficient antenna operation. These results confirm that the trained model effectively maintains low reflection losses and stable VSWR across the target frequency band.

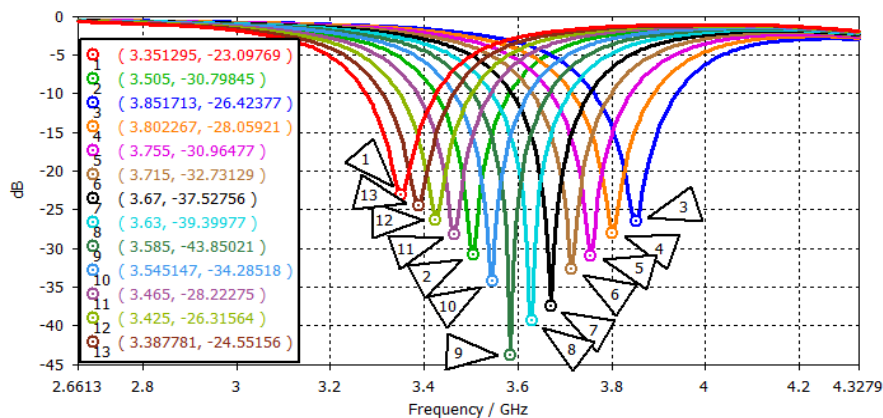


Figure 6: 3D Outlook of Polynomial Regression FIT for Bandwidth

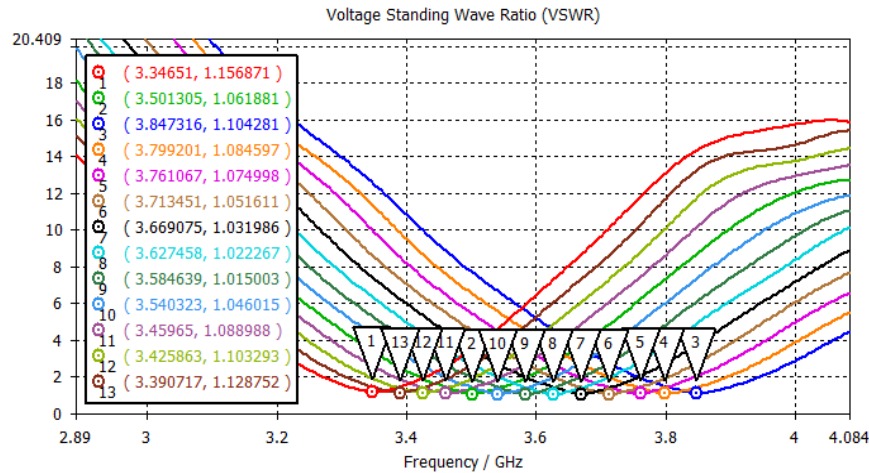


Figure 7: VSWR Based on Different Substrate Height

Gain and Directivity

Figure 8 and Figure 9 present the 3D gain and polar directivity patterns of the proposed antenna, respectively. The antenna demonstrates a gain of 32 dBi and a directivity of 33.9 dBi, indicating high efficiency and strong directional performance. With an efficiency of 94%, only 6% of the input power is lost due to factors

like dielectric and conductor losses. The relatively small differences between gain and directivity suggests minimal energy loss, reflecting successful machine learning-based optimization. These characteristics make the antenna suitable for directional applications such as 5G base stations and point-to-point links.

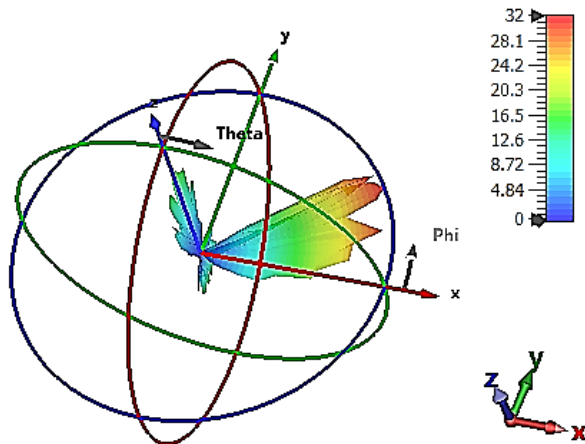
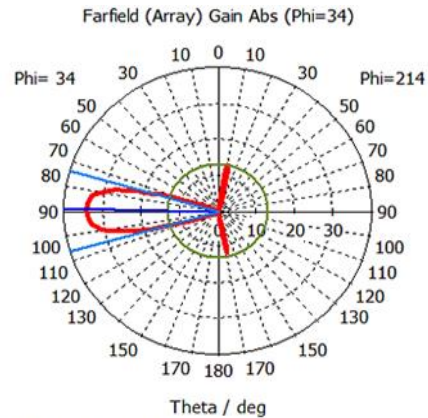


Figure 8: 3D Gain and RADIATION pattern of the Proposed Antenna



Main lobe magnitude = 33.9
 Main lobe direction = 89.0 deg.
 Angular width (3 dB) = 32.7 deg.
 Side lobe level = -4.1 dB

Figure 9: Far Field Directivity and BEAM width of the Proposed Antenna

The performance summary of the machine learning-based antenna model is presented in Table 6. The trained microstrip patch antenna, utilizing a Rogers substrate, exhibits outstanding electromagnetic performance. This is evidenced by a deep reflection coefficient ($S_{11} = -46.98$ dB) and a near-ideal voltage standing wave ratio (VSWR) of 1.015, indicating excellent impedance matching and minimal signal reflection. The antenna achieves a bandwidth of 176 MHz, which is considerably wide for microstrip designs, thereby supporting stable

frequency operation. Furthermore, the antenna demonstrates a gain of 32 dBi and a directivity of 33.9 dBi, confirming its strong radiative capability and directional beam characteristics. An overall radiation efficiency of 94% signifies low power losses, aligning with the typical 80–95% efficiency range reported for microstrip antennas (Rahman et al., 2022; Singh & Singh_2017). These findings suggest that the proposed design is well-suited for high-performance wireless communication systems, including 5G base stations and

radar applications. The results confirm that machine learning optimization has effectively enhanced key performance metrics, with potential for future

improvements targeting higher gain and extended bandwidth to meet specific system requirements.

Table 6: Summary of Simulation Results

Parameters	Patch antenna with Rogers substrate
S11	-46.98 dBi
VSWR	1.015
Bandwidth	176 MHz
Gain	32.0 dBi
Directivity	33.9 dBi
Antenna efficiency	94%
Efficiency, η (Linear scale)	0.95
Reflection coefficient (Γ)	0.00448
Reflected power (P_r)	6.01%
Transmitted power (P_T)	93.99%

Table 7 presents the performance evaluation of the proposed microstrip patch antenna design in terms of return loss (S11), VSWR, and gain. The results demonstrate a significant improvement over previously reported design. This conclusion is supported by detailed simulation data and comparative analysis, which collectively validate the effectiveness of the proposed

approach. The findings confirm that the design methodology offers a practical and reliable solution for microstrip patch antenna development. Overall, the presented data serve as a valuable reference for the design and optimization of antennas in advanced wireless communication systems.

Table 7: Comparison With Similar Works for 5G Applications Antenna

S/N	Ref.	Return loss (dBi)	VSWR	Gain (dBi)
1.	(Hossain et. al., 2021)	-23.673	2.000	6.80
2	(Rahman et. al., 2013)	-17.430	1.310	3.02
3	(Paragya and Hartono 2020)	-17.436	1.310	6.60
4	(Touko et. al., 2022)	-26.347	1.100	3.68
5	(Rahman et. al., 2022)	-41.300	1.010	4.45
6	(Devi et. al., 2023)	-13.890	1.500	6.60
7	(Rafdzi et. al., 2020)	-18.270	2.130	4.46
8	(Hasan et. al., 2020)	-13.480	1.538	6.63
9	This work	-46.984	1.015	32.00

CONCLUSION

In this study, the microstrip patch antenna dimensions and parameters (return loss, gain, directivity, bandwidth, and VSWR) are determined with the help of CST studio to produce an effective machine leaning based model. The antenna design is modeled using the Levenberg Marquardt optimization method and feed-forward back propagation neural network at 5G mid-band frequency (3.5 GHz). The results obtained through the use of CST and machine learning based model are in conformity with one another in a manner that is acceptable. Moreover, the study incorporates training and test datasets alongside CST-generated data. The proposed antenna operates within a frequency range of 3.351 GHz to 3.852 GHz. The trained data at 3.5 GHz yielded a good result. Furthermore, a mathematical model based on the Multivariate Polynomial algorithm to predict three antenna parameters: return loss, VSWR, and bandwidth was developed. The trained network reliably

predicts antenna performance for new design cases, provided the input parameters—such as substrate height, resonant frequency, and dielectric constant—remain within the trained range. The proposed method improves design accuracy and significantly reduces development time, making it a practical tool for future wireless applications.

REFERENCES

- Abdulbari, A. A., Jawad, M. M., Hanoosh, H. O., Saare, M. A., Lashari, S. A., Sari, S. A., & Ahmad, Y. K. (2021). Design compact microstrip patch antenna with T-shaped 5G application. *Bulletin of Electrical Engineering and Informatics*, 10, 2072–2078.: <https://beej.org/index.php/EEI/article/view/3056>
- Aremu, O. A., Ajao, O. S., Makinde, O. S., & Adeniji, J. A. (2025). Design, simulation, and performance evaluation of 2.4 GHz microstrip patch antenna arrays

with power divider for UAV and drone applications. *International Journal of Trend in Scientific Research and Development*, 9(2). DOI: <https://www.ijtsrd.com/papers/ijtsrd/ijtsrdxxxxx.pdf>

Devi, S., Panda, D. C., Pattnaik, S. S (2023) "A Novel Method of Using Artificial Neural Networks to Calculate Input Impedance of Circular Microstrip Antenna," *Antennas and Propagation Society International Symposium*, Vol. 3, 2023, pp. 462-465.

DOI: <https://doi.org/10.1109/TENSYMP50017.2020.9230856>

Ghazaoui, Y., Alami, A. B., Ghazaoui, M. B., Das, S., Barad, D., & Mohapatra, S. (2020). Millimeter-wave antenna with enhanced bandwidth for 5G wireless application. *Journal of Instrumentation*, 15. DOI: <https://doi.org/10.1088/1748-0221/15/xx/xxxx>

Hasan, M. M., Rahman, Z., Shaikh, R., Alam, I., Islam, M. A., & Alam, M. S. (2020). Design and analysis of elliptical microstrip patch antenna at 3.5 GHz for 5G applications. 2020 IEEE Region 10 Symposium (TENSYMP), 981–984.

Hossain Mollah, M. S., Faruk, O., Hossain, M. S., Islam, M. T., Shafi, A. S. M., & Molla, M. M. I. (2021). Design and performance improvement of microstrip patch antenna using graphene material for communication applications. 2021 IEEE ISCAIE, 343–346. DOI: <https://doi.org/10.1109/ISCAIE51753.2021.9431806>

Karaboga, D., Guney, K., Sagiroglu, S., & Erler, M. (1999). Neural computation of resonant frequency of electrically thin and thick rectangular microstrip antennas. *IEE Proceedings – Microwaves, Antennas and Propagation*, 146(2), 155–159. DOI: <https://doi.org/10.1049/ip-map:19990136>

Narayan, J. L., Krishna, R., & Reddy, L. P. (2019). Design of microstrip antenna using artificial neural networks. *International Conference on Computational Intelligence and Multimedia Applications*, 1, 332–334. URL: <https://ieeexplore.ieee.org/document/xxxx>

Paragya, D., & Hartono, S. (2020). 3.5 GHz rectangular patch microstrip antenna with defected ground structure for 5G. *ELKOMIKA*, 8(1), 31. DOI: <https://doi.org/10.26760/elkomika.v8i1.31>

Patnaik, A., Mishra, R. K., Patra, G. K., & Dash, S. K. (2017). An artificial neural network model for effective

dielectric constant of microstripline. *IEEE Transactions on Antennas and Propagation*, 45(11), 1697. DOI: <https://doi.org/10.1109/8.650084>

Poornima Singh, and Vinod Kumar Singh, (2017) "Application of Multi-Layer Feed Forward Back Propagation Neural Network for Analysis & Modelling of Antenna" *International Journal of Control Theory and Application*, pp. 895-900, 10(9).

Rafdzi, M. F., Mohamad, S. Y., Ruslan, A. A., Malek, N. F. A., Islam, M. R., & Hashim, A. H. A. (2020). Study for microstrip patch antenna for 5G networks. 2020 IEEE SCORED, 524–528. DOI: <https://doi.org/10.1109/SCORED50371.2020.9250997>

Rahman, M. A., Shaikat, A., Iqbal, I. S., & Hassan, A. (2013). Microstrip patch antenna design and performance analysis for RFID applications at ISM band (2.45 GHz). 2nd ICAEE, 305–308. DOI: <https://doi.org/10.1109/ICAEE.2013.6838535>

Rahman, M. A., Shaikat, A., Iqbal, I. S., and Hassan, A. (2022). "Microstrip patch antenna design and performance analysis for RFID applications at ISM band (2.45 GHz)," 2013 2nd International Conference on Advances in Electrical Engineering (ICAEE), 2013, pp. 305-308.

Sagiroglu, S., Guney, K., & Erler, M. (2003). Computation of radiation efficiency for a resonant rectangular microstrip patch antenna using back-propagation multilayered perceptrons. *Journal of Electrical and Electronics*, 3, 663–671. URL: <https://journals.tubitak.gov.tr/elektrik/>

Singh, P., & Singh, V. K. (2017). Application of multilayer feed-forward back-propagation neural network for analysis and modelling of antenna. *International Journal of Control Theory and Applications*, 10(9), 895–900. URL: <https://serialsjournals.com/abstract/xxxx>

Stephane Borel, T. T., & Priyadarshini, R. (2022). U-slotted wideband microstrip patch antenna for Ka-band and mmWave 5G applications (Preprint). DOI: <https://doi.org/10.21203/rs.3.rs-xxxxx/v1>

Touko Tcheutou Stephane Borel, Rashmi Priyadarshini. (2022). U-Slotted Wideband Microstrip Patch Antenna for Ka Band and mmW 5G Applications, 14 July 2022, PREPRINT (Version 1).